度及紫外屏蔽的橡仁粉/卡拉胶基可胶&热封的油脂包装膜的制备及性能研究

迟文锐[1] 宁语苹[1] 刘文华[1] 刘若婷[1] 李坚[1] 王立娟[1]*

（1. 东北林业大学 哈尔滨 150000）

摘 要：塑料的大量使用造成了白色污染，使生态环境被严重破坏。治理和消除白色污染已成为全球的共同目标。因此，研制出可生物降解的包装薄膜材料迫在眉睫。天然聚合物，如多糖和蛋白质，可用来生产包装膜并具有代替合成聚合物的潜力。目前，已有很多比传统塑料包装膜具有更好的阻隔性、抗菌性或抗氧化性的多糖基薄膜被研制出来。但由于多糖的熔融温度高于热解温度导致其无法通过热封形成有效地包装袋，难于实际应用。淀粉和蛋白质衍生的薄膜可热封并用作塑料的替代品。然而，这种利用方式可能会加剧全球粮食短缺。本研究中，我们利用废弃的橡子与卡拉胶制备了可胶&热封的复合包装膜。测试了橡仁粉/κ-卡拉胶（AKM/κC）复合膜的机械强度，热稳定性，透光率，雾度和抗菌性能。结果表明，当甘油从30%增加到 50%时，雾度和透光率分别从 96.74%和 3.50%下降到 94.50%和 2.25%。AKM/κC 薄膜具有优异的紫外线屏蔽性能（380-200 nm 处的透过率为 0）。使用 15g/L 的壳聚糖季铵盐（CQAS）作为生物胶水对 45g-AKM/κC 薄膜进行胶&热封。在 115 ºC，0.3MPa 下热封 1s 的密封强度最大，为 5.09±0.29N/15mm。用 45g-AKM/κC 包装的牛油在 25 ºC 贮存 75 天后，过氧化值（POV）从 0.0187 g/100g 增加到 0.0336 g/100g，低于暴露在空气中的牛油的 POV（0.5209 g/100g，已变质）。我们制备的薄膜具有较高的雾度和紫外线屏蔽性能，可用作富含脂肪食品的塑料包装替代品。

关 词：橡仁粉；κ-卡拉胶；复合膜；高雾度；紫外屏蔽；可密封

Fabrication and characterization of a glue- and heat- sealable acorn kernel meal/κ-carrageenan composite film with high-haze and UV-shield for packaging grease

Abstract: The extensive utilization of plastics has resulted in the emergence of white pollution, which poses a severe threat to the ecological environment. Consequently, tackling and eradicating this issue has become a shared objective worldwide. Therefore, it is imperative to expedite the development of biodegradable packaging film materials. Natural polymers, such as polysaccharides and proteins, possess the potential to replace synthetic polymers in producing packaging films. Numerous polysaccharide-based films have been developed with better barrier, antimicrobial or antioxidant properties compared to traditional plastic packaging films. However, their practical application is limited due to they pyrolze before melting which hinders heat-sealing for effective bag formation. Starch- and protein-based films are viable substitutes for plastics, as they can be heat-sealed. However, the utilization of starches and proteins in this way may exacerbate global food shortages. In this study, we used discarded acorns to prepare a glue- and heat-sealable packaging film. We evaluated the mechanical characteristics, thermal stability, transmission, haze, and antimicrobial properties of an acorn kernel meal/κ-carrageenan (AKM/κC) composite film. The results showed that the haze and transmittance decreased from 96.74% to 94.50% and from 3.50 to 2.25%, respectively, when glycerol increased from 30% to 50%. The AKM/κC film had excellent UV shielding properties (transmittance at 380-200 nm was 0). The 45 g-AKM/κC films were sealed through a comnination of bio-glue composed of 15 g/L chitosan quaternary ammonium salt (CQAS) and heat at 115 ºC for 1 s under a pressure of 0.3 MPa, resulting in a maximum sealing strength of 5.09 ± 0.29 N/15 mm. Beef tallow packaged in 45g-AKM/κC exhibited an increased peroxide value (POV) from 0.0187 to 0.0336 g/100 g after 75 days of storage at 25 oC, which was lower than that in air (0.5209 g/100g, which has deteriorated).

基金项目：黑龙江省自然科学基金（ZD2020C003）

*王立娟为通讯作者

Our developed film had high haze and UV shielding performance and can be used as a plastic packaging substitute for fat-rich foods.

Key words: acorn kernel meal; κ-Carrageenan; composite film; high-haze; UV-shield; sealability.

1 Introduction

Plastics are widely used in packaging due to their low-cost, stability, light weight and durability; however, plastics do not decompose contributing to environmental pollution (Cárdenas-Alcaide et al., 2022; Shen et al., 2020). Plastic pollution has become a global problem that urgently requires a solution (Chu et al., 2023; Walker and Fequet, 2023). A viable solution is to replace plastics with renewable biomass (Mohamed et al., 2020). Natural polymers, which possess adequate film-forming ability, such as chitosan (El Mouzahim et al., 2023), sodium alginate (Guo et al., 2023), pectin (Xie et al., 2023), cellulose (Huang et al., 2022a), hemicelluloses (Peng and She, 2014), carrageenan (Han et al., 2023), soybean isolate protein (Liu et al., 2021) and starch (Ortega et al., 2023) , etc., are potential plastic substitutes for packaging. For example, chitosan and curry leaf essential oil have been used as packaging materials with insect repellency (Nazurah et al., 2022). Sodium alginate film and Clitoria ternatea extract have been used to maintain and monitor food freshness (Santos et al., 2022). Citron peel pectin and glycerol as a plasticizer has been developed into a superior food packaging film via a response surface method (Asfaw et al., 2023). Waste cotton textiles and tea polyphenols have been used to produce transparent cellulose-based films with antibacterial, antioxidant and UV resistance properties (Xia et al., 2022). κ-Carrageenan and mulberry polyphenol extracts were mixed to prepared a packaging film with pH-responsive and antioxidant properties (Liu et al., 2019). Even though these food packaging films have better properties such as oxygen barrier, antimicrobial or antioxidant than traditional plastic packaging, they are not used in food packaging because polysaccharide-based films can't be heat-sealed into bags due to the fact that they pyrolyze before melting (Chi et al., 2023b). Starch- and protein-derived films have been heat-sealed into bags. For instance, soybean isolate protein-based films incorporated with diatomite/thymol complex were used to package blueberries for extended shelf life (Lu et al., 2021). Chicken protein isolate/fish gelatin composite film containing phenolic compounds was used to package chicken skin oil via heat sealing (Nilsuwan et al., 2021). However, those proteins are not only key nutrients for human health (Rawiwan et al., 2022), but they are also troublesome to extract and expensive. Sago starch-based film can be formed into bags by heat-sealing with a sealing strength of 375 N/m (Abdorreza et al., 2011). Cassava starch-based films were used to package pork and retard its spoilage (Katekhong et al., 2022). These starches are derived from staple foods; hence, the use of these foods for the preparation of plastic substitutes might exacerbate the global food shortage (Botreau and Cohen, 2020). Therefore, there is a need for a starch-rich biomass that can be used as a plastic substitute.

Starch-rich acorns are the fruit of oaks. China has an annual yield of 6 to 7 million metric tons starch-rich acorns (Chao et al., 2017). However, it is barely eaten or even fed to livestock in most areas of China, which is due to the acorn kernels content plenty of tannins with astringent flavor and anti-nutrients (Pasqualone et al., 2019). As a result, acorns are discarded (Sardão et al., 2021). Acorn kernel is an ideal film-forming biomass; its tannin content might contribute UV-shielding properties to the film (Huang et al., 2022b). Tannins were incorporated into sodium alginate/silk protein film that exhibited exceptional UV-blocking capabilities (Zhang et al. 2023). The nanocomposite films of Eucommia ulmoides rubber containing Fullerene C60 exhibited a 100% shielding effect against the UV light (Wei et al., 2021). A chitosan film blended with low molecular weight poly(limonene) also

demonstrated outstanding UV shielding properties (Goncalves et al., 2023). The incorporation of acorn kernel meal (AKM) containing tannins as a direct raw material would streamline the film preparation process by eliminating the need for additional UV shielding agents. Nonetheless, starch-based films are often brittle and have poor mechanical properties, which can be improved by adding more hygroscopic κ-carrageenan, which is a linear anionic polysaccharide composed of galactose and dehydrated galactose extracted from red algae (Jiang et al., 2023; Wang et al., 2023). Our previous study has suggested that κ-carrageenan film could be glue-sealed into bags by electrostatic action (Chi et al., 2023b). Currently, there is no report on AKM blended with κ-carrageenan (κC) to prepare a glue- and heat-sealable food packaging film.

In this study, we investigated the effect of glycerol addition on AKM/κC composite films. We further studied the films using scanning electron microscopy (SEM), Fourier-transform infrared (FTIR) spectroscopy, and thermogravimetric analysis (TGA). We measured light transmittance, haze, oxygen permeability (OP), water vapor permeability (WVP), mechanical properties. We selected 45g-AKM/κC to investigate the heat-sealing parameters and used it to package beef tallow.

2. Materials and methods

2.1. Materials

Acorn was acquired from Anguo Fangcaojia Trading Co., Ltd. (Baoding, China). κC was purchased from Qingdao Bairen Biotechnology Co., Ltd. (Shandong, China). Chitosan quaternary ammonium salt (CQAS) was bought from Nantong Lushen Biological Engineering Co., Ltd (Jiangsu, China). Glycerol was offered by Yongda Chemical Co., Ltd. (Tianjin, China). Beef tallow was obtained from a local market (Harbin, China).

2.2. Methods and equipment

2.2.1 Determination of components in AKM

The 180 mesh AKM was obtained by milling the acorns after peeling, cleaning and drying. The starch, tannin, lipid, protein and fiber contents in the AKM were determined according to Chinese GB 5009.9-2016 (the 1st method: enzymatic hydrolysis), Chinese GB 5848-86, Chinese GB 5009.6-2016 (the 1st method: soxhlet extraction), Chinese GB 5009.5-2016 (the 2nd method: spectrophotometry) and Chinese GB 5009.10-2003, respectively.

2.2.2 Preparation of films

AKM (6.0 g, dry weight) was dispersed into 200 mL of distilled water (room temperature) and then stirred at 80 °C for 30 min. Subsequently, κC (20%, w/w of AKM basis) was added and stirred for 30 min. Glycerol (30%, 35%, 40%, 45%, 50%, w/w of AKM basis) was incorporated into the AKM/κC solution and further stirred for 30 min. Finally, the mixture was poured into a mould (30.0 cm × 29.0 cm × 4.0 cm) and dried about 12 h at 50 °C. The obtained films were denoted as 30g-AKM/κC, 35g-AKM/κC, 40g-AKM/κC, 45g-AKM/ κ C and 50g-AKM/κC corresponding to the glycerol amounts.

2.2.3 Characterizations

Morphologies of the AKM and the cross section of the films were photographed by a SEM of Apreo S Hivac (Thermo Fisher Scientific Inc, USA). FTIR spectra of κC, AKM and films were recorded by a Nicolet iN10 spectrometer (Thermo Fisher Scientific Inc, USA) within the wavenumber from 550 to 4000 cm-1. The thermostability of glycerol and films were performed via a Q500 thermogravimetric analyzer (TA Company, USA)

from 20 °C to 600 °C under 10 °C /min in N2. The gelatinization temperature of 45g-AKM/κC was measured after adequate wetting using a Q2000 differential scanning calorimeter (TA Instruments – Water LLC, USA) from 30 °C to 160 °C under a nitrogen atmosphere at a heating rate of 10 °C /min. The haze (400~700 nm) and light transmittance (200~800 nm) of films were obtained via a haze mater (CS-700, CHNSpec, China) and spectrophotometer (UV-2600, Shimadzu, Japan), respectively.

2.2.4. Performance measurements

The OP of the films with 33% RH and 53% RH was measured via an oxygen transmission rate tester (OX/230, Labthink, China). The WVP of the films under 75% RH (25 °C) was obtained using the gravimetric method. The average thickness of the films was randomly obtained at 240 points by an ID-C112XBS micrometer (Mitutoyo Corp., Japan). After the rectangular films (1.5 cm × 8.0 cm) were conditioned at 25 °C with different humidity (11% RH, 33% RH, 53% RH and 75% RH) for 48 h, the TS and EB were detected by an auto-tester (XLW-PC, Labthink, China) with a strain rate of 30.0 cm/min. Each sample was examined in 4 replicas. The bacteriostatic activity of the film was assessed via plate counts. 9 mL of bacterial suspension (10000 CFU/mL, E. coli or S. aureus) was cocultured with 0.2 g of broken films in a constant temperature shaker incubator at 37 °C for 4 h. Afterwards, 0.2 mL of the mixture was evenly coated on nutrient agar medium and cultured at 37 °C for 1 d. Finally, the count of colonies on the nutrient agar medium was recorded using an automatic colony counter (lcont-50, Xunda Technology Co., Ltd., China). A control experiment was carried out without broken film addition. The bacteriostatic rate of the films can be calculated by Eq. (1):

$$\text{Bacteriostatic rate} = (C-X)/C \times 100\% \quad (1)$$

where C and X are the colony counts of the control experiment and the experiment, respectively..

2.2.5. Synergized glue- and heat-sealing strength measurement

Rectangular 45g-AKM/κC (7.5 cm × 11.5 cm) was glue and heat synergistically sealed using a heat seal tester (AT-RF, Anmc, China). 0.2 mL of 15 g/L CQAS solution was coated along a 1.0 cm width of overlap of the two rectangular edges and pressure sealed at 0.10~0.40 MPa and 100~120 °C for 0.8~1.2 s. For measurement of sealing strength, the sealed film was cut to 1.5 cm × 6.5 cm and then stored at 33% RH for 12 h. The glue- and heat-sealing strength were measured by using an XLW-PC electronic tensile machine (Labthink, China) at a strain rate of 5 mm/s. Four replicates of each sample were tested.

2.2.6. Packaging beef tallow

A square 45g-AKM/κC (12.0 cm × 12.0 cm) was folded in half, CQAS solution was coated on the 1.0 cm width of the remaining edge, and the pressure sealed for 1.0 s at 0.30 MPa and 115 °C using a heat seal tester to result a bag contain 10.0 g of beef tallow. After storage at 25 °C for 75 days, the beef tallow was taken out and measured the peroxide value (POV) by following Chinese GB 5009.227-2016 (Titration method). Triplicate measurements of each sample were performed.

2.2.7. Statistics analysis

The SPSS v17.0 (SPSS Inc., USA) was utilized for data analysis with the Duncan multiple range test ($P < 0.05$).

3. Results and discussion

3.1. Acorn kernel meal component analysis

AKM contains 86.18±0.02% starch, 7.90±0.22% tannin, 2.47±0.04% lipids, 0.92±0.03% protein, and 0.13±0.00% fiber (Table 1). Starch and tannin can provide favorable heat sealability and UV shielding for AKM-based films, respectively.

Table 1. Content of components in AKM.

Sample	Starch (%)	Tannin (%)	Lipids (%)	Protein (%)	Fiber (%)
AKM	86.18±0.02	7.90±0.22	2.47±0.04	0.92±0.03	0.13±0.00

3.2. AKM and films morphology

Fig. 1 shows the morphology of AKM and the AKM/κC composite film by SEM. The AKM granules were irregular, polygonal and elliptical with some voids and debris on the surface could be observed in Fig. 1 (a). The AKM/κC composite film presented several pits and protrusions (Fig. 1 b~f) formed by the lipids evaporation during high vacuum. Similar results were observed in composite films of black corn seed powder/κC (Chi et al., 2023a) and olive pomace/chitosan (de Moraes Crizel et al., 2018). Tannin and proteins form precipitates that uniformly disperse in the composite films (Khongkliang et al., 2023). After quenching in liquid nitrogen, random pits and protrusions were formed in the cross-sections of the films. Furthermore, with increasing glycerol addition, these particles became smaller and more numerous. It is possible that glycerol prevented their aggregation during the film-forming and drying processes.

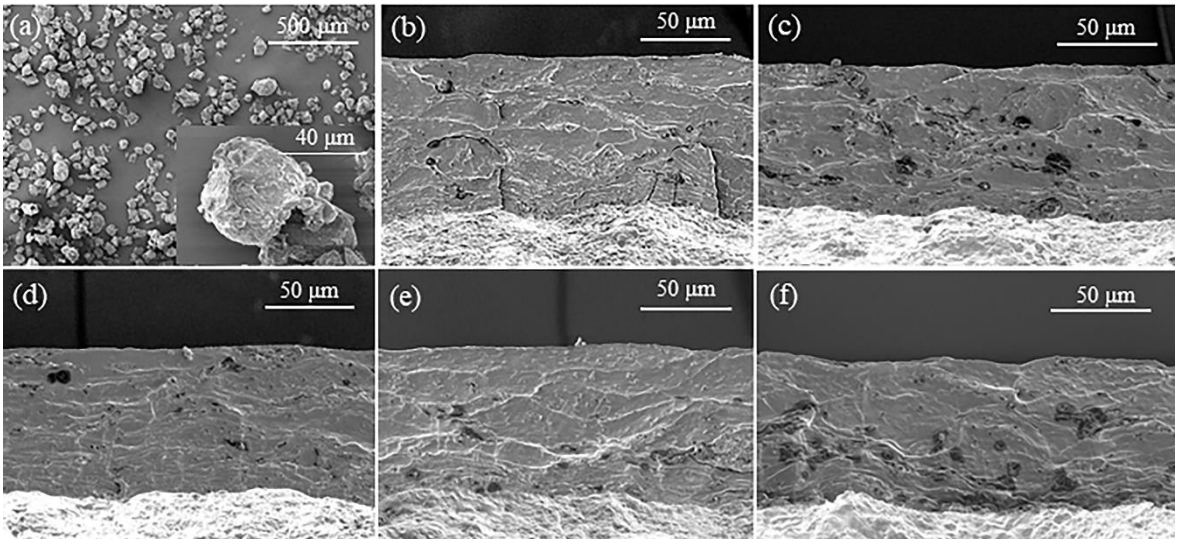

Fig. 1 SEM images of AKM (a), cross-sections of 30g-AKM/κC (b), 35g-AKM/κC (c), 40g-AKM/κC (d), 45g-AKM/κC (e) and 50g-AKM/κC (f).

3.3. FTIR analysis

Fig. 2 shows the FTIR spectra of κC, AKM and composite films. Bands at 3305, 2924, 2853 and 1638 cm-1 are associated with the O–H and N–H stretching vibrations, C–H stretching vibrations, C–H bending vibrations, and water absorption, respectively (Daoud et al., 2019; Sun et al., 2019). In κC, the bands at 1230 cm-1, 925 cm-1 and 842 cm-1 are attributed to sulfate ester, 3,6-anhydrogalactose and galactose-4-sulfate ester, respectively (Ili Balqis et al., 2017). AKM displayed the bands at 1742 cm-1 (C=O of lipids) and 1240 cm-1 (N–H from protein)

(Rozenberg et al., 2019). Those bands could be easily observed in the composite film spectra (Fig. 2 b). The intensity of the band at 3305 cm-1 increased with the addition of glycerol, which might be caused by glycerol obstructed regeneration of starch. Furthermore, there were no significant differences in the spectra of the composite films, demonstrating that no chemical reaction occurred among the components in the films. The deconvolution spectra of AKM and composite films are illustrated in Fig. 2 (c, d). The intensities of ~1040 cm-1 and ~995 cm-1 are correlated with starch crystalline phases, whereas intensity of ~1020 cm-1 is associated with the amorphous phase (Chen and Sopade, 2013). The 995/1020 and 1040/1020 ratios can be evaluated the starch crystallinity; higher ratios suggest a more crystalline structure. The absorption intensity of AKM was slightly higher at 995 cm-1 than at 1020 cm-1, and 995/1020 ratio was 1.03. That for AKM/κC composite films were less than 1.03, and the band at 1040 cm-1 disappeared. This result might be attributed to the fact that κC and glycerol prevent the starch retrogradation during the films formation process, thereby reducing crystallinity. When glycerol increased from 30% to 50%, the 995/1020 ratio decreased from 0.94 to 0.86, which suggested the amorphous region of starch in the composite films increased. This result (Fig. 2d) was consistent with those in Fig. 2 (b).

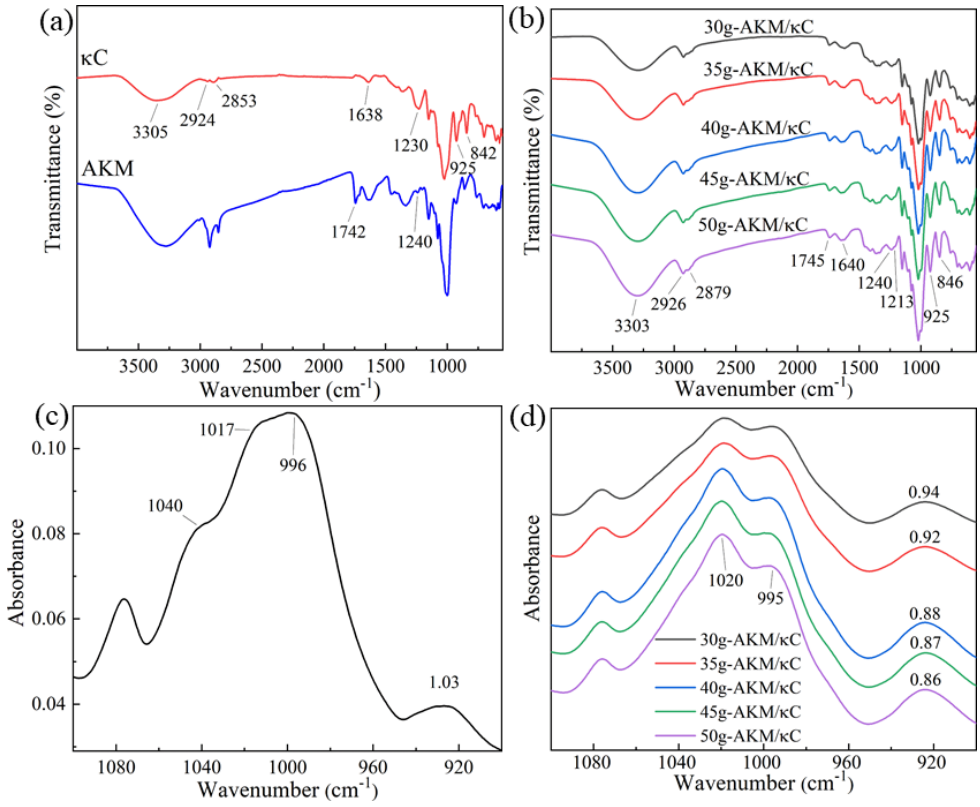

Fig. 2 Original (a,b) and deconvoluted (c,d) FTIR spectra of κC, AKM and composite films.

3.4. Optical performance and antibacterial activity

Fig. 3 (a, b) presents the optical performance of the composite films. When glycerol addition increased from 30% to 50%, transmittance decreased from 3.50% to 2.25%. According to SEM images, the particles in the composite film became smaller and more numerous with increasing glycerol addition, which resulted in more reflection as light pass through the film. In addition, the composite films have excellent UV shielding (0% transmittance at 200-380 nm), which is due to the tannin with abundant phenolic hydroxyl groups that can adsorb

UV (Huang et al., 2022b). The composite film haze decreased from 96.74% to 94.50%, due to glycerol that reduced the regeneration of starch. This speculation is supported by FTIR result. The antibacterial properties of the composite films are shown in Fig. 3 (c). The bacteriostatic effects of composite film against E. coli and S. aureus decreased from 66.09% to 11.40% and from 56.63% to 27.63%, respectively, when glycerol increased from 30% to 50%. With increasing glycerol addition, the content of tannin, which possess antibacterial properties, decreases. The composite films had a stronger antibacterial effect against S. aureus than E. coli.

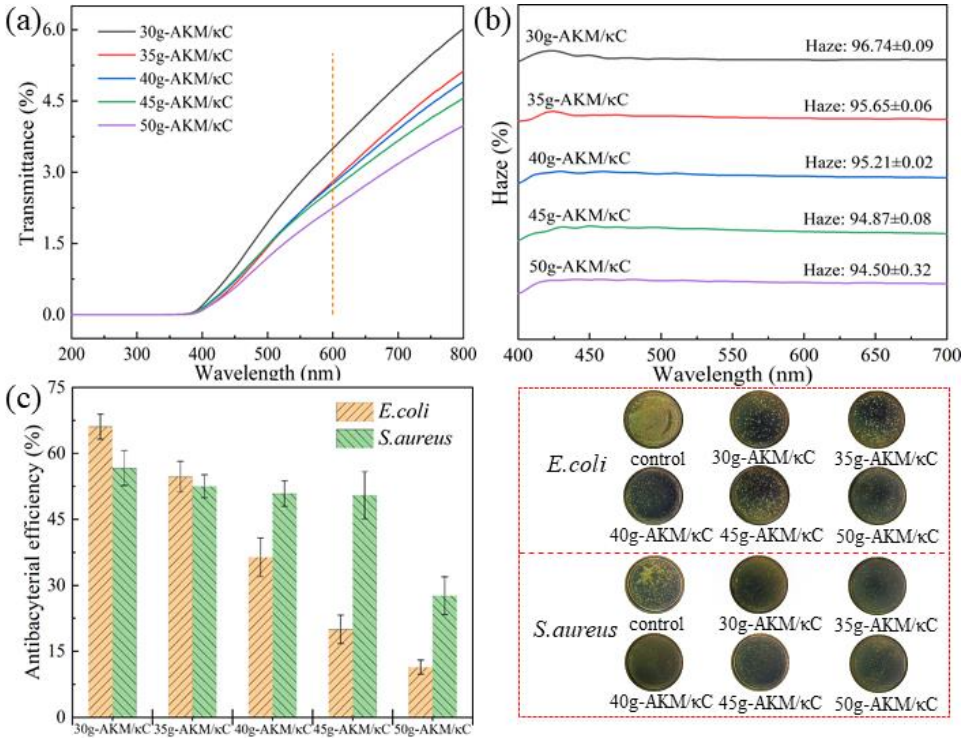

Fig. 3 Optical performance (a:transmittance, b:haze) and antibacterial properties of the composite film (c).

3.5. Physical properties

Thickness, WVP, OP and moisture content of the composite films are presented in Table 2. The thickness, WVP and OP increased with glycerol content. It was possible that glycerol disrupted the dense structure of the polymers, created more space. The increase in WVP may also be related to more hydroxyl groups (evidenced by the FTIR spectra). Similar results have been obtained in several researches (Cao et al., 2018; Gomes et al., 2022; Sun et al., 2018). OP increased with humidity, because moisture acted as a plasticizer, further weakening the film structure. Moisture content increased with glycerol addition; the highly hydrophilic glycerol increased the hydrophilicity of the composite film. The space between the polymers contributed to more water. In addition, composite films had a higher moisture content at a higher relative humidity.

Table 2. Thickness, WVP, OP and moisture content of the composite films.

Samples	Thickness (mm)	WVP (g m^{-1} s^{-1} Pa^{-1}×10^{-}	Moisture Content (%)				OP (cm^3 mm m^{-2} day^{-1} atm^{-}	
			11%RH	33%RH	53%RH	75%RH	35%RH	53%RH
30g-AKM/κC	0.088±0.007a	0.91±0.03a	8.38±0.58a	10.73±0.80a	15.76±0.44a	27.17±1.75a	3.43±0.68a	445.29±1.00a
35g-AKM/κC	0.091±0.010b	1.02±0.08a	10.52±0.21b	13.79±0.17b	18.31±0.12b	30.56±0.30b	29.68±0.98b	476.65±11.05a

40g-AKM/κC	0.093±0.009c	1.28±0.11b	11.56±0.13c	16.90±0.34c	21.39±0.85c	32.57±0.35b	44.86±2.74c	566.00±15.61b
45g-AKM/κC	0.095±0.009c	1.73±0.04c	16.17±0.05d	18.81±0.90d	24.94±0.65d	35.02±0.69c	84.47±2.83d	840.50±26.27c
50g-AKM/κC	0.098±0.007d	1.81±0.02c	18.12±0.17e	22.50±0.59e	26.17±0.37e	38.32±1.05d	163.28±1.32e	1354.87±2.71d

Fig. 4 (a) shows the monthly average absolute humidity in 34 major cities in China from 2009 to 2018 (www.weather.com.cn). In this study, we measured the mechanical properties of the composite films in a humidity range (11% to 75% RH) that is representative of 70% of major cities in China. As shown in Fig. 4 (b), the EB of the composite films increased with the content of glycerol and moisture, which was attributed to easier slide between polymers caused by plasticizers. The EB of 50g-AKM/κC at 75% RH was lower than that at 53% RH, which was due to fewer hydrogen bonds between polymers resulting in an easier fracture of the composite film. At lower relative humidity (11% RH), the TS of the composite film was determined by a combination of intermolecular hydrogen bonding of the polymers and film flexibility. At 30% glycerol, the film was brittle and susceptible to fracture, resulting in a low TS. At 45% glycerol, TS increased from 1.53±0.18 to 18.95±0.85 MPa, which was due to increased flexibility, causing the films to withstand more tensile strength. At 50% glycerol, the intermolecular hydrogen bonds decreased, thereby reducing TS to 9.81±0.67 MPa. In addition, the TS of the composite film decreased with increased glycerol and moisture content at RH ≥ 33%. This can be explained by a reduction in hydrogen bonding between the polymers due to glycerol and moisture. Therefore, we used 45g-AKM/κC for subsequent research, due to its better mechanical properties at lower humidity (11% RH).

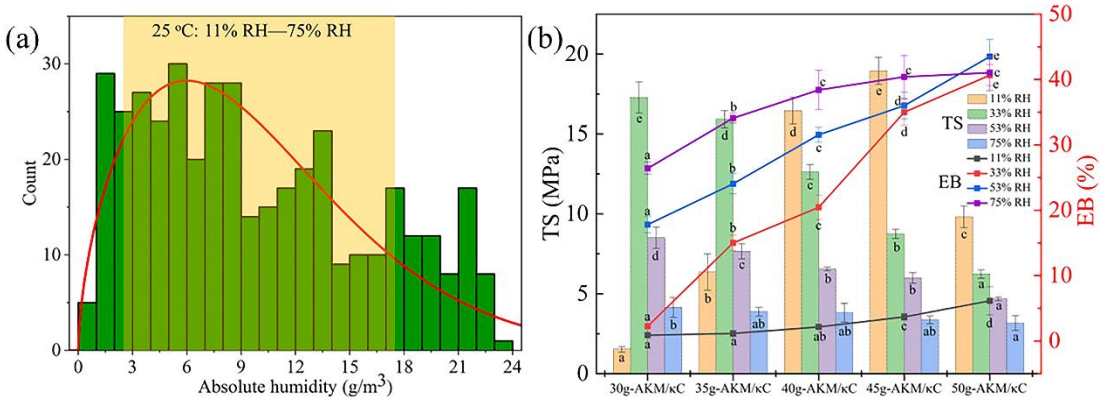

Fig. 4 Data distribution of the average monthly absolute humidity in 34 major cities in China from 2009-2018 (www.weather.com.cn, a); TS and EB of the composite films at different relative humidity (b).

3.6. Thermal stability

The thermogravimetric analysis of glycerol and AKM/κC composite films are illustrated in Fig. 5 (a, b). The weight loss of glycerol at 125-220 °C could be attributed to its evaporation. The composite film had three weight loss stages. The first stage below 100 °C was ascribed to the evaporation of water. The second stage resulted from the evaporation of glycerol, consistent with the results on glycerol-plasticized cassia gum film (Cao et al., 2018). The third stage was the pyrolysis of polysaccharides. In addition, when glycerol increased from 30% to 50%, pyrolysis temperature decreased from 262.56 °C to 257.97 °C. It is likely that glycerol disrupted the polymer interactions, thereby reducing the thermal resistance of the composite films. Similar results were obtained by using glycerol to plasticize the Dioscorea hispida starch film (Hazrati et al., 2021). Fig. 5 (c) shows that the gelatinization

temperature of 45g-AKM/κC ranged from 98.87 to 144.77 °C, indicating that the composite film could be heat-sealed.

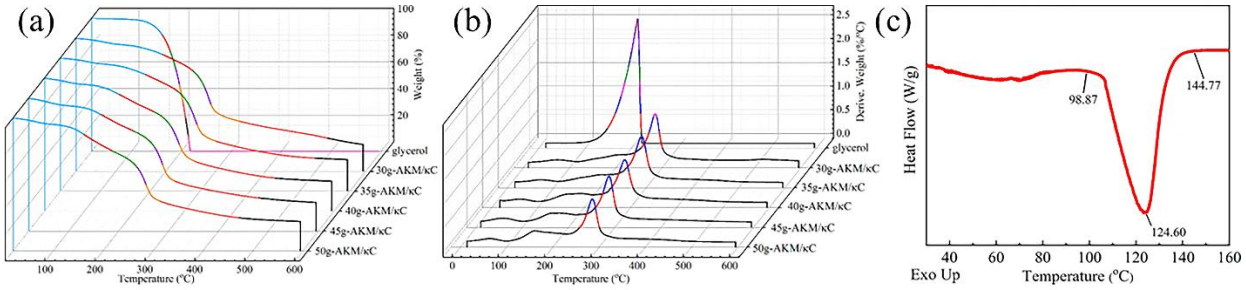

Fig. 5 TGA (a) and DTG (b) of glycerol and the composite film, and DSC of 45g-AKM/κC (c).

3.7. Synergistic heat & glue-sealing property

Fig. 6 (a) shows the variations in the sealing strength of 45g-AKM/κC at different heat-sealing temperature and time with 0.3 MPa of heat-sealing pressure. With prolonged heat-sealing time (1.2 s) or high heat-sealing temperature (120 °C), sealing strength decreased probably due to the thinning of the heat-sealing area. In addition, the fracture mode was Ⅱ at 1.2 s (except at 115 ° C), which may be due to the non-uniform bonding between the layers of the heat-sealing region by the combined effect of heat-sealing temperature and time. At 0.8 s and 100 ° C, the fracture mode was Ⅰ, which may be due to weak bonding in the heat-sealing area. The fracture mode was Ⅲ at 115 ° C, indicating that the strength of the bond in the sealed region is higher than that of the film. Fig. 6 (b) presents the variations in sealing strength of the composite film with heat-sealing pressure for different heat-sealing time at 115 °C. The sealing strength of 45g-AKM/κC increased with pressure because the appropriate pressure promotes the bonding of the heat-sealing layers. However, with increasing pressure, the sealing area became thinner, resulting in a reduction in heat-sealing strength. Sealing strength reached a maximum value of 5.09±0.29 N/15 mm at 115 °C and 0.3 MPa for 1 s. As shown in Fig. 6 (d), both CQAS and heat could seal the composite film. The glue-sealing strength of 45g-AKM/κC was lower than the heat-sealing strength, which was attributed to the lower κC content. Moreover, sealing strength of 45g-AKM/κC was > 2 N/15 mm for either sealing method, which is satisfactory for daily use according to Chinese GB/T 10003-2008.

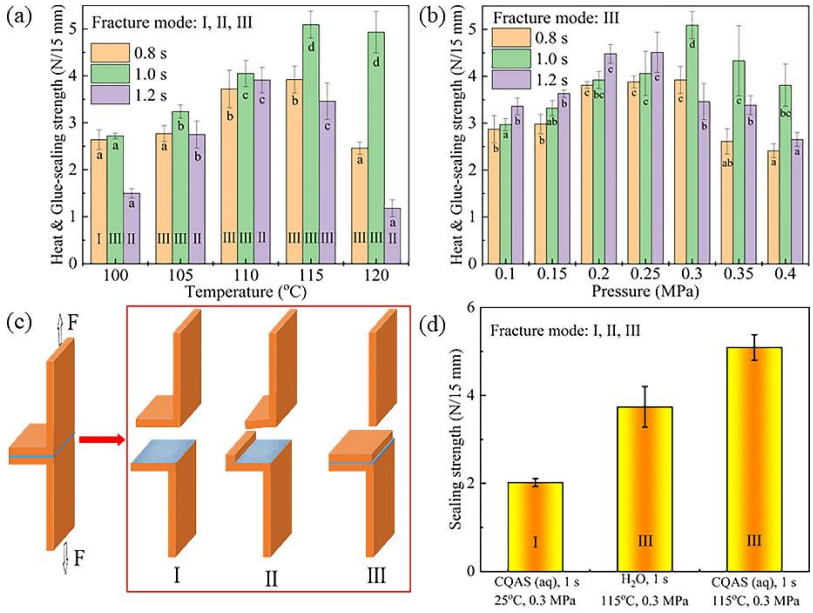

Fig. 6 Effect of heat-sealing temperature (a) and pressure (b) on the sealing strength of composite films at different heat-sealing time; Facture mode (c); Effect of heat and CQAS on sealing strength (d).

3.8. Application in packaging beef tallow

Beef tallow is susceptible to rancidity during storage because it is rich in unsaturated fatty acids. Fig. 7 (b) shows that the air-exposed beef tallow had spoiled after 75 d since the POV rose from 0.0187 to 0.5209 g/100 g. The POV of beef tallow packaged in 45g-AKM/κC and PE film corresponded 0.0336 and 0.1035 g/100 g, showing that both hadn't spoiled. Compared with our previous research (Chi et al., 2023b), the POV of beef tallow packaged in 45g-AKM/κC increased by 79.68%, while that of beef tallow packaged in κC film increased by 627.55% after storage of the same days. This is probably explained by the delayed oxidation of beef tallow in the composite film with excellent UV resistance. Therefore, 45g-AKM/κC has the potential to be used as a material for packaging fat-rich food.

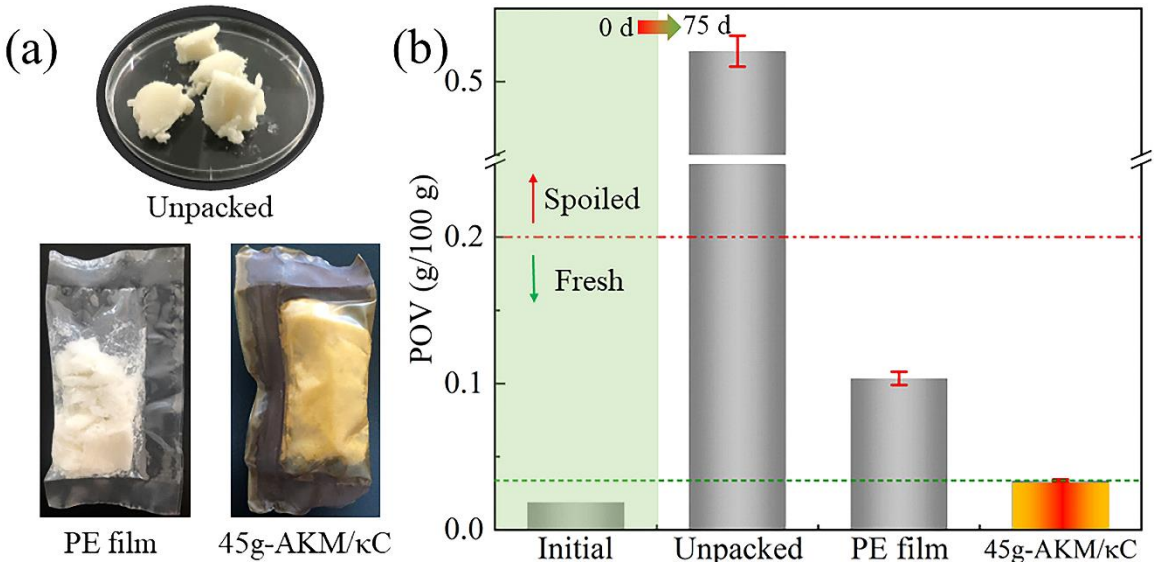

Fig. 7 Images of beef tallow exposed to air and packaged with PE film and 45g-AKM/κC (a), and POV before and after 75 d

(b).

4. Conclusions

We used acorns to prepare a glue- and heat-sealable AKM/κC composite film with high haze and UV resistance. AKM has good compatibility with κC. With increased glycerol, thickness, OP, and WVP increased, but light transmission, haze, thermal stability, and antimicrobial properties decreased. With increased humidity, oxygen barrier decreased and flexibility increased. The glue- and heat-sealing strength of 45g-AKM/κC was 5.09±0.29 N/15 mm at 0.3 MPa for 1 s (115 °C). After 75 days, exposed beef tallow had 15.5× the POV of beef tallow packaged in 45g-AKM/κC, indicating that 45g-AKM/κC was effective in extending the shelf life of grease. Our glue- and heat-sealable biomass-based film can be a substitute to plastic packaging. Additionally, our study provides a novel method for utilizing acorns.

References

Abdorreza, M.N., Cheng, L.H., Karim, A.A., 2011. Effects of plasticizers on thermal properties and heat sealability of sago starch films. Food Hydrocolloids. 25, 56-60.

Asfaw, W.A., Tafa, K.D., Satheesh, N., 2023. Optimization of citron peel pectin and glycerol concentration in the production of edible film using response surface methodology. Heliyon. 9, e13724.

Botreau, H., Cohen, M.J., 2020. Gender inequality and food insecurity: A dozen years after the food price crisis, rural women still bear the brunt of poverty and hunger. Advance in Food Security and Sustainability. 5, 53-117.

Cao, L., Liu, W., Wang, L., 2018. Developing a green and edible film from Cassia gum: The effects of glycerol and sorbitol. Journal of Cleaner Production. 175, 276-282.

Cárdenas-Alcaide, M.F., Godínez-Alemán, J.A., González-González, R.B., Iqbal, H.M.N., Parra-Saldívar, R., 2022. Environmental impact and mitigation of micro(nano)plastics pollution using green catalytic tools and green analytical methods. Green Analytical Chemistry. 3, 100031.

Chao, B., Liu, R., Zhang, X., Zhang, X., Tan, T., 2017. Tannin extraction pretreatment and very high gravity fermentation of acorn starch for bioethanol production. Bioresource Technology. 241, 900-907.

Chen, G., Sopade, P., 2013. In vitrostarch digestion in sweet potato (Ipomoea batatas L.) flours. International Journal of Food Science & Technology. 48, 150-156.

Chi, W., Liu, W., Li, J., Wang, L., 2023a. Simultaneously realizing intelligent color change and high haze of kappa-carrageenan film by incorporating black corn seed powder for visually monitoring pork freshness. Food Chemistry. 402, 134257.

Chi, W., Liu, W., Xu, S., Zhan, X., Li, J., Wang, L., 2023b. A new strategy to glue-seal κ-carrageenan film for packaging grease. Journal of Food Engineering. 337, 111248.

Chu, J., Zhou, Y., Cai, Y., Wang, X., Li, C., Liu, Q., 2023. Flows and waste reduction strategies of PE, PP, and PET plastics under plastic limit order in China. Resources, Conservation and Recycling. 188, 106668.

Daoud, S., Bou-Maroun, E., Dujourdy, L., Waschatko, G., Billecke, N., Cayot, P., 2019. Fast and direct analysis of oxidation levels of oil-in-water emulsions using ATR-FTIR. Food Chemistry. 293, 307-314.

de Moraes Crizel, T., de Oliveira Rios, A., D. Alves, V., Bandarra, N., Moldão-Martins, M., Hickmann Flôres, S., 2018. Active food packaging prepared with chitosan and olive pomace. Food Hydrocolloids. 74, 139-150.

El Mouzahim, M., Eddarai, E.M., Eladaoui, S., Guenbour, A., Bellaouchou, A., Zarrouk, A., Boussen, R., 2023. Food packaging composite film based on chitosan, natural kaolinite clay, and Ficus. carica leaves extract for fresh-cut apple slices preservation. International Journal of Biological Macromolecules. 233, 123430.

Gomes, V., Pires, A.S., Mateus, N., de Freitas, V., Cruz, L., 2022. Pyranoflavylium-cellulose acetate films and the glycerol effect towards the development of pH-freshness smart label for food packaging. Food Hydrocolloids. 127, 107501.

Goncalves, S., Barbosa, M., Júnior, L., Alves, R., Vieira, R., 2023. Poly(limonene): A novel renewable oligomeric antioxidant and UV-light blocking additive for chitosan-based films. Food Packaging and shelf Life. 37, 101085.

Guo, Q., Yuan, Y., He, M., Zhang, X., Li, L., Zhang, Y., Li, B., 2023. Development of a multifunctional food packaging for meat products by incorporating carboxylated cellulose nanocrystal and beetroot extract into sodium alginate films. Food Chemistry. 415, 135799.

Han, Y., Zhou, M., McClements, D.J., Liu, F., Cheng, C., Xiong, J., Zhu, M., Chen, S., 2023. Investigation of a novel smart and active packaging materials: Nanoparticle-filled carrageenan-based composite films. Carbohydrate Polymers. 301, 120331.

Hazrati, K.Z., Sapuan, S.M., Zuhri, M.Y.M., Jumaidin, R., 2021. Effect of plasticizers on physical, thermal, and tensile properties of thermoplastic films based on Dioscorea hispida starch. International Journal of Biological Macromolecules. 185, 219-228.

Huang, K., Maltais, A., Liu, J., Wang, Y., 2022a. Wood cellulose films regenerated from NaOH/urea aqueous solution and treated by hot pressing for food packaging application. Food Bioscience. 50, 102177.

Huang, X., Ji, Y., Guo, L., Xu, Q., Jin, L., Fu, Y., Wang, Y., 2022b. Incorporating tannin onto regenerated cellulose film towards sustainable active packaging. Industrial Crops and Products. 180, 114710.

Ili Balqis, A.M., Nor Khaizura, M.A.R., Russly, A.R., Nur Hanani, Z.A., 2017. Effects of plasticizers on the physicochemical properties of kappa-carrageenan films extracted from Eucheuma cottonii. International Journal of Biological Macromolecules. 103, 721-732.

Jiang, C., Liu, T., Wang, S., Zou, Y., Cao, J., Wang, C., Hang, C., Jin, L., 2023. Antioxidant and ammonia-sensitive films based on starch, kappa-carrageenan and Oxalis triangularis extract as visual indicator of beef meat spoilage. International Journal of Biological Macromolecules. 235, 123698.

Katekhong, W., Wongphan, P., Klinmalai, P., Harnkarnsujarit, N., 2022. Thermoplastic starch blown films functionalized by plasticized nitrite blended with PBAT for superior oxygen barrier and active biodegradable meat packaging. Food Chemistry. 374, 131709.

Khongkliang, P., Khemkhao, M., Mahathanabodee, S., S, O.T., Kadier, A., Phalakornkule, C., 2023. Efficient removal of tannins from anaerobically-treated palm oil mill effluent using protein-tannin complexation in conjunction with electrocoagulation. Chemosphere. 321, 138086.

Liu, K., Xu, X., Liu, H., Liu, Z., Zhao, K., Ma, Y., Zhang, K., 2021. Mechanical properties and water sensitivity of soybean protein isolate film improved by incorporation of sodium caseinate and transglutaminase. Progress in Organic Coatings. 153, 106154.

Liu, Y., Qin, Y., Bai, R., Zhang, X., Yuan, L., Liu, J., 2019. Preparation of pH-sensitive and antioxidant packaging films based on kappa-carrageenan and mulberry polyphenolic extract. International Journal of Biological Macromolecules. 134, 993-1001.

Lu, J., Li, T., Ma, L., Li, S., Jiang, W., Qin, W., Li, S., Li, Q., Zhang, Z., Wu, H., 2021. Optimization of heat-sealing properties for antimicrobial soybean protein isolate film incorporating diatomite/thymol complex and its application on blueberry packaging. Food Packaging and Shelf Life. 29, 100690.

Mohamed, S.A.A., El-Sakhawy, M., El-Sakhawy, M.A., 2020. Polysaccharides, Protein and Lipid -Based Natural Edible Films in Food Packaging: A Review. Carbohydrate Polymers. 238, 116178.

Nazurah, R.N.F., Noranizan, M.A., Nor-Khaizura, M.A.R., Nur Hanani, Z.A., 2022. The potential of chitosan-based film with curry leaf essential oil as natural insect-repellent food packaging. Food Packaging and Shelf Life. 34, 100993.

Nilsuwan, K., Arnold, M., Benjakul, S., Prodpran, T., de la Caba, K., 2021. Properties of chicken protein isolate/fish gelatin blend film incorporated with phenolic compounds and its application as pouch for packing chicken skin oil. Food Packaging and Shelf Life. 30, 100761.

Ortega, F., Minnaard, J., Arce, V.B., García, M.A., 2023. Nanocomposite starch films: Cytotoxicity studies and their application as cheese packaging. Food Bioscience. 53, 102562. https://doi.org/10.1016/j.fbio.2023.102562.

Pasqualone, A., Makhlouf, F.Z., Barkat, M., Difonzo, G., Summo, C., Squeo, G., Caponio, F., 2019. Effect of acorn flour on the physico-chemical and sensory properties of biscuits. Heliyon. 5, e02242.

Peng, P., She, D., 2014. Isolation, structural characterization, and potential applications of hemicelluloses from bamboo: A review. Carbohydrate Polymers. 112, 701-720.

Rawiwan, P., Peng, Y., Paramayuda, I.G.P.B., Quek, S.Y., 2022. Red seaweed: A promising alternative protein source for global food sustainability. Trends in Food Science & Technology. 123, 37-56.

Rozenberg, M., Lansky, S., Shoham, Y., Shoham, G., 2019. Spectroscopic FTIR and NMR study of the interactions of sugars with proteins. Spectrochimca Acta Part A: Molecular and Biomolecular Spectroscopy. 222, 116861.

Santos, L.G., Alves-Silva, G.F., Martins, V.G., 2022. Active-intelligent and biodegradable sodium alginate films loaded with Clitoria ternatea anthocyanin-rich extract to preserve and monitor food freshness. International Journal of Biological Macromolecules. 220, 866-877.

Sardão, R., Amaral, R.A., Alexandre, E.M.C., Saraiva, J.A., Pintado, M., 2021. Effect of high-pressure processing to improve the safety and quality of an Quercus acorn beverage. Lwt. 149, 111858.

Shen, M., Song, B., Zeng, G., Zhang, Y., Huang, W., Wen, X., Tang, W., 2020. Are biodegradable plastics a promising solution to solve the global plastic pollution?. Environmental Pollution. 263, 114469.

Sun, G., Chi, W., Zhang, C., Xu, S., Li, J., Wang, L., 2019. Developing a green film with pH-sensitivity and antioxidant activity based on κ-carrageenan and hydroxypropyl methylcellulose incorporating Prunus maackii juice. Food Hydrocolloids 94, 345-353.

Sun, G., Liang, T., Tan, W., Wang, L., 2018. Rheological behaviors and physical properties of plasticized hydrogel films developed from κ-carrageenan incorporating hydroxypropyl methylcellulose. Food Hydrocolloids. 85, 61-68.

Walker, T.R., Fequet, L., 2023. Current trends of unsustainable plastic production and micro(nano)plastic pollution. TrAC Trends in Analytical Chemistry. 160, 116984.

Wang, C., Cao, J., Liu, T., Jin, L., Hang, C., Zhang, C., Qian, X., Jiang, D., Jiang, C., 2023. Preparation and characterization of antioxidant and pH-sensitive films based on arrowhead (Sagittaria sagittifolia) starch, kappa-carrageenan and black chokeberry (Aronia melanocarpa) extract for monitoring spoilage of chicken wings. International Journal of Biological Macromolecules. 224, 544-555.

Wei, X., Yang, X., Ma, A., Zhang, J., Peng, P., Dong, J., 2021. Fullerene C60/Eucommia ulmoides rubber nanocomposite films with excellent UV-blocking performance for controlling wheat scab fungus. Industrial Crops and products. 162, 113301.

Xia, G., Ji, X., Xu, Z., Ji, X., 2022. Transparent cellulose-based bio-hybrid films with enhanced anti-ultraviolet, antioxidant and antibacterial performance. Carbohydrate Polymers. 298, 120118.

Xie, J., Zhang, Y., Klomklao, S., Simpson, B.K., 2023. Pectin from plantain peels: Green recovery for transformation into reinforced packaging films. Waste Management. 161, 225-233.

Zhang, X., Kang, J., Hu, H., Wang, H., Liu, Z., Zhou, W., Zhang, X., 2023. Impacts of tannin inclusion on fabrication, characterization and antioxidant activity of sodium alginate-silk fibroin-tannin films and their application on fresh-cut apple packaging. Food Bioscience. 54, 102897.